Available free online at www.medjchem.com

Mediterranean Journal of Chemistry **2018**, 6(6), 238-254

Application of Commercial Adsorbent for Rare earth elements - Uranium Mutual Separation and Purification

Ahmed. H. Orabi [1,*], Kamal A. Rabia [1], Elsayed E. Elshereafy [2] and Amany R. Salem [1]

[1] Nuclear Materials Authority, P.O. Box 530, El Maadi, Cairo, Egypt

[2] Chemistry Dept., Faculty of Science, Minoufia University, Cairo, Egypt

Abstract: The treatment of rare earths sulfate liquor contaminated with traces of uranium as radioactive contaminates utilizing lewatit mono plus M500 was studied. Adsorption behavior was studied by batch experiments to determine the optimum conditions for uranium removal. The obtained equilibrium data were found to be satisfactory fitted with Langmuir isotherm and the second order rate equation. Also, elution process was achieved by 2M NaCl/1M HCl solution and the reuse of sorbent remains appreciable. A marketable pure product of rare earth oxide was prepared in addition to pure sodium diuranate containing total uranium content of the starting REEs cake.

Keywords: uranium separation; lewatit mono plus M500; purification of REEs concentrate; monazite.

Introduction

There were a spacious assortment rare earth minerals known, but notably, the most important source minerals were bastnaesite (La, Ce)FCO_3, monazite, (Ce, La, Th)PO_4, and xenotime, YPO_4. Thorium and too much less extent uranium were generally associated with the lanthanides and their assay in monazite attain 5 to 6% and <1 respectively [1-6]. The other kind of rare earth resources, mainly found in China, was clayed minerals such as kaolin, feldspar, and mica [7-10]. Uranium and thorium contents in these resources were found to be about 20–30 ppm based on total rare earth oxide [11, 12].

In Egypt, 15% heavy economic minerals (ilmenite, rutile, magnetite, zircon, and monazite) were distributed along the beaches of the northern parts of the Nile Delta from Rosetta to Damietta [13, 14]. Sulfuric acid and alkali caustic soda was used for processing monazite [15-17]. The former method was more used and also applied in a pilot plant in NMA project to produce a monazite sulfate solution of U, Th, and REEs while silica, zircon or other admixed gangue minerals are left insoluble.

The wide range of rare earths in the industrial application was relied upon their chemical, catalytic, electrical, magnetic, and optical properties. Rare earths were widely used for local industries, scientific research, High-technology and nuclear power [6, 18 – 25].

The methods of rare earth recovery from a variety of resources have gained much interest. The rare earths were associated usually with radioactive elements of uranium and thorium which contaminate it. The separation of uranium and thorium from the earth elements represented the big concern in rare earth industry to avoid environmental pollution and the contamination of rare earth products [26, 27]. Uranium, if it can be recovered economically as a by-product, may be usable as nuclear fuel.

Many variety methods were used for recovery of pure mixed REEs as well as Th and U products from the sulfuric acid breakdown method [14]. Abdelfattah, et al., 2014 were suggested separation of the REEs by direct application of a cation exchange resin upon the monazite sulfate liquor after adding hydrazine sulfate reductant to reduce Ce (IV) to its trivalent state [28]. However, complete separation of such pure products by these methods was generally difficult and would require another excessive manipulation and in turn relatively high costs. Ganser et al., 2014; Lockyer, 2014 suggested that ion exchange (IX) was used to remove a small amount of thorium and uranium in the rare earth chloride and sulphate solutions. But, the used resin was not revealed and no detailed test work was reported for uranium recovery in the process [29, 30]. D2EHPA and EHEHPA were used for separation of uranium from rare earths. However, the stripping of U(VI) and Th(IV) from them was difficult [31, 32].

It was found that good separation between uranium and thorium in nitrate solutions was achieved when using synthesized amide. Since these reagents

**Corresponding author: Ahmed. H. Orabi*
Email address: a_orabi_chem@yahoo.com
DOI: http://dx.doi.org/10.13171/mjc66/01712211014-orabi

Received November 16, 2017
Accepted, December 3, 2017
Published December 21, 2017

were not commercially available, no practical application has been found [33].

This research focused on the separation of uranium from rare earths concentrate, produced after sulphuric acid processing of Egyptian monazite mineral, to produce high purity of rare earths and uranium concentrate.

Experimental

Reagents

All chemicals were of analytical reagent grade, used without further purification, and supplied from Merck. The strong base industrial grade lewatit mono plus M500 ion exchange resin was essentially a macroreticular anion exchange resin that has been used in the present work to determine its equilibrium and kinetic characteristics for uranium (VI) recovery from a rare earths solution. It was washed with distilled water followed by 0.5 M sulfuric acid for several times in turn and was then dried at 50°C. The characteristics of lewatit mono plus M500 were suggested in Table 1.

Table 1. Characteristics of the ion exchange resin.

Resin	LEWATIT MonoPlus M 500
Physical form	Yellow translucent spherical beads
Matrix	cross-linked poly strene
Fonctional group	quaternary amine
Ionic form	as shipped Cl^-
Moisture holding capacity (wt %)	48–55 (Cl^- form)
Shipping weight (g/L)	690
Particle size (mm)	0.62
Uniformity coefficient	1.1(max)
Reversible swelling (Max vol %)	$Cl^- \rightarrow OH^-$ 20
Maximum operating temperature (°C)	70

Material preparation

The REEs liquor used in this experiment was produced through monazite digestion with concentrated sulfuric acid in a closed reactor with continuous stirring. The digestion reaction results in a thick grey paste was cooled, diluted with water for about twenty times the weight of the mineral and stirred for at least 2 hour. Cooling has to be maintained in order to prevent the temperature from rising above 17°C; the solubility of the rare earth sulfates increased as the temperature was decreased. The prominent advantage of the sulfuric acid method was that it can be used for all types and grades of commercial monazite and does not require fine grinding [34, 35]. By this treatment, all rare earths go into a solution which was decanted out from silica, rutile, zircon, and the unreacted monazite that easily settled down in few hours. The hydrated thorium oxide was first precipitated by neutralization with ammonia to a pH 0.9. Rare earths were then precipitated from the filtrate by careful neutralization to pH 2.5 as shown in (Fig. 1).

The obtained rare earth precipitate is converted into the corresponding mixed hydrous oxides by boiling with sodium hydroxide in a stoichiometric ratio for 1 hour.

Batch sorption studies

100 g from the produced rare earth concentrate, contaminated with uranium (200 ppm), was dissolved in diluted sulfuric acid. In order to study the relevant factors affecting the recovery process of uranium from high rare earths concentration, many series of batch technique experiments were performed. These experiments were performed by shaking 1g sample portions of lewatit mono plus M500 with 100 mL rare earth solution (200 U mg/L). The studied factors involve; pH, contact time, initial uranium concentration, and temperature. The adsorption efficiencies of uranium were calculated by the difference between its equilibrium and initial concentrations as the following equation:

$$(RE)_2(SO_4)_3.(NH_4)_2SO_4.2H_2O + 8NaOH \longrightarrow 2RE(OH)_3.2H_2O + 2NH_4OH + 4Na_2SO_4 \quad (1)$$

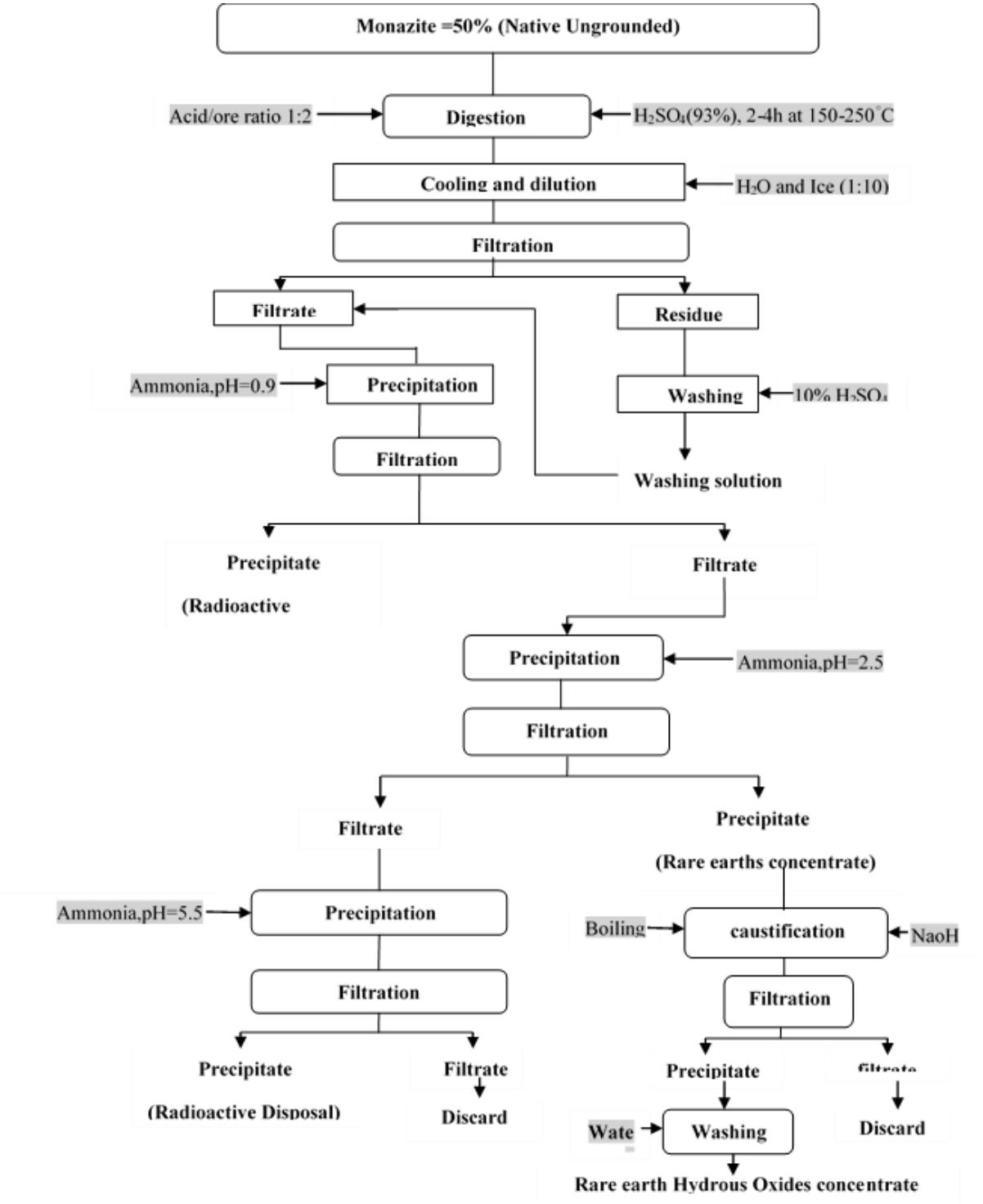

Figure 1. A flow diagram for processing of Egyptian crude monazite with concentrated sulfuric acid

The adsorption efficiency (Ads%) and adsorption capacity (q) were calculated as:

$$q = \left(\frac{(C_i - C_f)}{m} \right) xV \quad (2)$$

$$Ads\% = \left(\frac{(C_i - C_f)}{Ci} \right) x100 \quad (3)$$

Where, C_i and C_f are the initial and the final concentrations of U in the aqueous phase, respectively. *m* is the weight of the adsorbent used (g) and V is the volume of the solution (L). For elution process, the loaded uranium was eluted from the lewatit mono plus M500, through applying a number of eluting agents with different concentrations together with different elution time.

In the adsorption cycle or step, the uranium anionic complexes are adsorbed on the resin according to the following reaction, where R^+ represents the fixed ion-exchange sites of the resin:

$$(R_4N^+)_2SO_4^{2-} + UO_2(SO_4)_2^{2-} \longrightarrow (R_4N^+)_2UO_2(SO_4)_2^{2-} + SO_4^{2-} \quad (4)$$

Analytical procedures

The major oxides in the obtained sulfuric acid solution of Rosetta monazite concentrate sample were determined using the conventional wet chemical technique of Shapiro and Brannock (1962) [36] thus, the SiO_2, TiO_2, and P_2O_5 were determined using their relevant spectrophotometric methods while the total Fe as Fe_2O_3 was determined by titrimetric methods using sulfosalicylic against EDTA solutions. Meanwhile, REEs and Th were spectrophotometrically determined by using the chromogenic reagent, Arsenazo-III [37]. Individual REEs were measured in the samples using prism ICP-OES, Teledyne technologies (Inductively Coupled Plasma Optical Emission Spectrometer). In the meantime, the purity of the final precipitate of the REEs and Th oxalate has qualitatively been determined using ESEM-EDX analysis. Analysis of U in the different aqueous stream solutions was fluorometrically determined by using the laser fluorometer "UA-3" [Uranium Analyzer (Scintrex, Canada)]. Also, the control analysis of uranium (VI) in the different solution streams has also been performed by the same method. All experiments were carried out three times, and only the average values were reported. The maximum errors were less than 3%.

Results and Discussion

Material characteristics

As previously mentioned, the working Egyptian crude monazite concentrate sample of about 50% purity was subjected to proper analysis. Results of the complete chemical analysis of the working sample are shown in Table 2.

Table 2. Major constituents of the input Egyptian Rosetta monazite raw material (50%).

Element oxide	Constituents %	RSD %
P_2O_5	**14.5**	**± 3.1**
RE_2O_3	**31.4**	**± 2.6**
ThO_2	**2.9**	**± 2.5**
U_3O_8	**0.33**	**± 3.76**
Insoluble Residue	**50**	**± 1.26**

The monazite was digested with sulfuric acid as illustrated in (Fig.1). The produced rare earths concentrate was normally and usually contaminated with uranium (200 ppm) and as a result, it must be subjected to purification probably by adsorption technique.

Optimization factors of uranium adsorption using lewatit mono plus M500 adsorbent

Optimization of the U adsorption conditions through various experimental conditions such as contact time, initial pH, U concentration, and temperature was illustrated as follow:

Effect of pH

The pH of the working media is the main factor for the recoveries of metal ions. The reason to explain the pH in solution has a strong influence on the metal solution chemistry as well as the ionic state of the functional groups on the surface of adsorbent [38]. The effect of pH on the adsorption of uranium on lewatit mono plus M500 was studied. 200 ppm U in each experiment (100 mL REEs sulfate liquor) was preconcentrated in the pH range of 1–2.5 by introducing on the 1 g resin and respective results were shown in Fig. 2. Uranium adsorption efficiency increased from 59.5% at pH 1 to a maximum value of 91.2% (pH 1.8) and then declines slowly from 91.2% to 84.25%. The bivalent and in particular the tetravalent uranium sulfate complexes (at lower PH) were found to have a high affinity for the anionic exchange resins [39, 40]. Then, pH 1.8 of the sample was selected for further experiments. The bivalent $[UO_2(SO_4)_2]^{2-}$ and in particular the tetravalent uranium sulfate complexes $[UO_2(SO_4)_3]^{4-}$ (at lower PH) were found to have a high affinity for the anionic exchange resins [39, 40]. On the other hand, after PH over 2 value, a respective value of REEs was found to captured with uranium may be due to their precipitation or some elemental hydrolyzation on the resin surface competing and or / inhibit uranium adsorption resin capacity resulting in complete uranium adsorption and impure REEs effluents (products). Then, pH 1.8 of the sample was selected for further experiments. In the adsorption cycle or step, the uranium anionic complexes are adsorbed on the resin and their interaction may be represented as follow, where R^+ represents the fixed ion-exchange sites of the resin, where R represents the inter-change medium resin and X^- equals sulfate anions.

$$[UO_2(SO_4)_2]^{2-}{}_{aq.} + 2RX \leftrightarrows R_2[UO_2(SO_4)_2] + 2X^-{}_{aq}$$

$$[UO_2(SO_4)_3]^{4-}{}_{aq.} + 4RX \leftrightarrows R_4[UO_2(SO_4)_3] + 4X^-{}_{aq.}$$

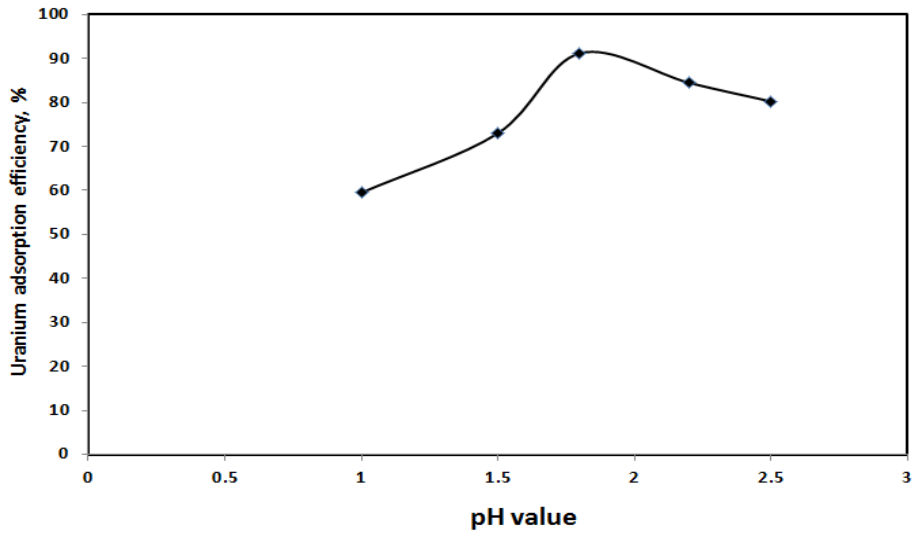

Figure 2. Effect of pH upon uranium adsorption efficiency from REEs sulfate liquor by lewatit mono plus M500

Effect of contact time

It is important to evaluate the contact time at which that the uranium is absorbed from aqueous solutions in order to design the treatment plant. To understand the effect of contact time on uranium adsorption onto lewatit mono plus M500, experiments were conducted with 100 mL REEs sulfate liquors having 200 U mg/L concentration with initial pH 1.8 at room temperature of 25°C using 1 g of adsorbent. The samples were analyzed after each experiment to estimate the concentration of dissolved uranium as a function of equilibration time. Fig. 3 shows that the process is characterized by a rapid adsorption in the first 30 min of equilibration time, followed by a slow process, leading to maximum adsorption in around 30 min. the increase in sorption amount of uranium with increasing time may be due to the increase of adsorbate quantity. The extent of uranium sorption decreases significantly with the increase of contact time, which is dependent on the decrease in the number of vacant sites on the surfaces of resin. Besides, after the lapse of some time, the remaining free surface sites are difficult to occupy due to the repulsive forces between the solute molecules on the solid surface and the bulk phase and this trend indicates that the sorbent is saturated at this level [41, 42], therefore 30 min shaking time was found to be appropriate and used in all subsequent experiments.

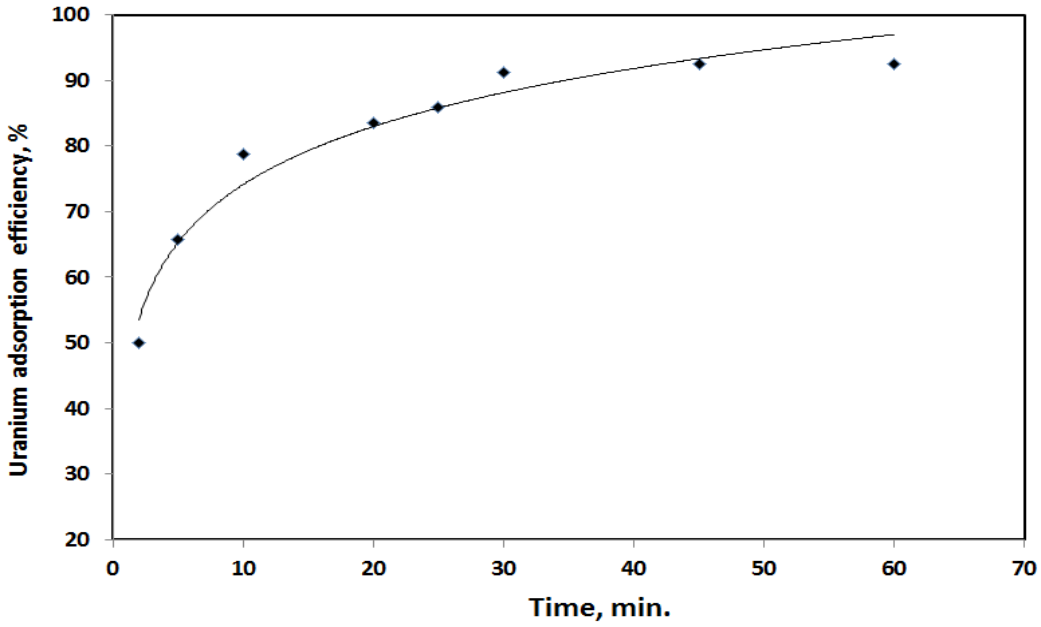

Figure 3. Effect of contact time upon uranium adsorption efficiency from REEs sulfate liquor by lewatit mono plus M500

Effect of adsorbent dosage

The relation between adsorbent dosage and adsorption efficiency has also been investigated. The volume of solution (100 mL), the concentration of uranium (200 mg/L), the pH of the solution (1.8) and the time of adsorption (30 min) were kept constant while the amount of resin varied from 0.5 to 2 g. As shown in Fig. 4, by increasing the amount of

adsorbent the adsorption percentage of uranium increases. The increase observed in adsorption due to increasing the amount of adsorbent could be attributed to the increase in surface area and the availability of adsorption [43]. While at a constant concentration, increasing adsorbent leads to more unsaturated sites which could be the reason why the amount of uranium adsorption per unit weight of adsorbent decreases.

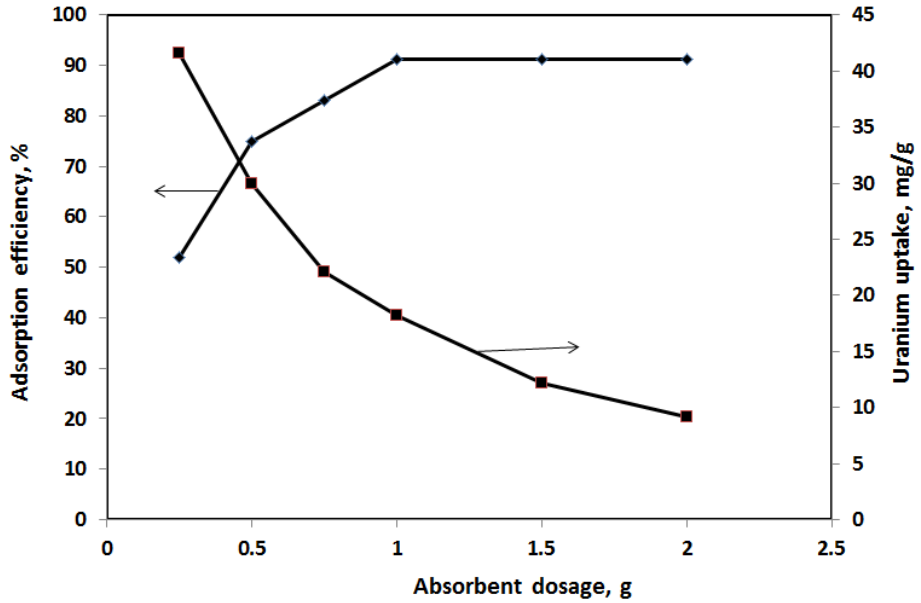

Figure 4. Effect of the adsorbent dose on uranium (VI) sorption by lewatit mono plus M500 resin. pH = 1.8, T = 25 °C, Time = 30 min, and Ci = 200 mg/L.

Effect of uranium concentration

The effect of initial uranium concentration on lewatit was studied by contacting a fixed mass of adsorbent (1gm) with a solution of 100 mL with initial pH 1.8 at room temperature of 25°C for 30 minutes with different concentration of uranium ranged from 100 up to 600 mg/L. Uranium adsorption efficiency decreased with increasing uranium initial concentration because the uranium amount increases with the same mass of lewatit mono plus M500 as shown in Fig. 5. Therefore, it can be ascertained that the maximum loading capacity of uranium from sulfate medium upon lewatit mono plus M500 is 35.5 mg/g equivalent to 35.5 g/Kg lewatit mono plus M500. From the scan electron microscopy (SEM) images of the studied resin before and after uranium(VI) adsorption are shown in Fig. 6 (a, b and c), respectively. The SEM images clearly seem the difference between the surfaces of the studied resin. Although a good uniformity and smooth surface are observed in the conventional resin but the surface after U(VI) adsorption is observed a brilliant spot on the resin beads. As could be seen from the results, a visible change of the surface morphology in the U(VI) adsorbed resin demonstrates that the sorption of U(VI) ions are taken place onto the resin.

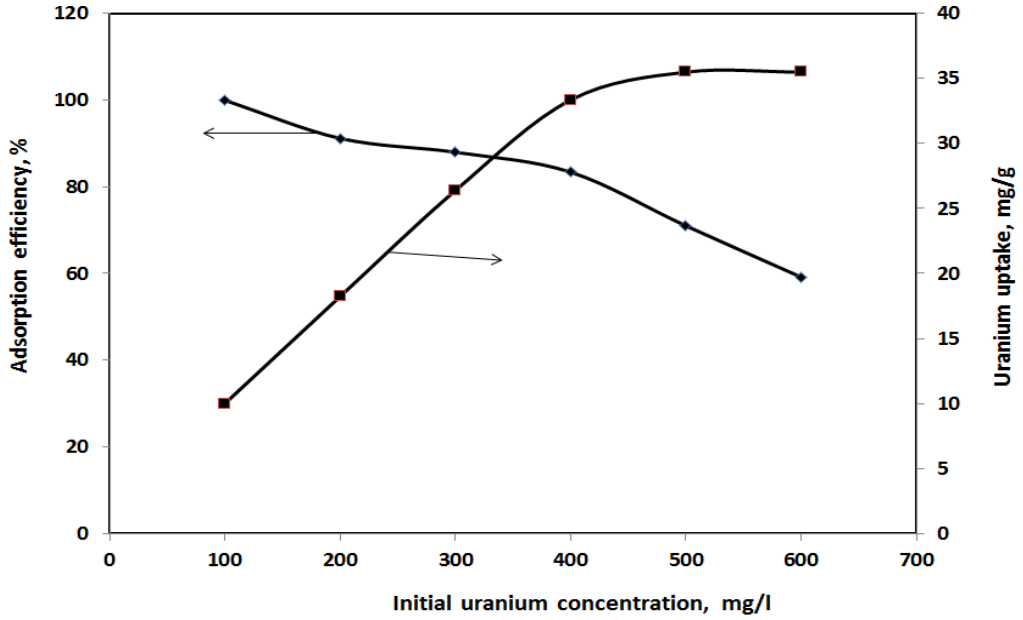

Figure 5. Effect of initial uranium concentrations on adsorption efficiency of lewatit mono plus M500

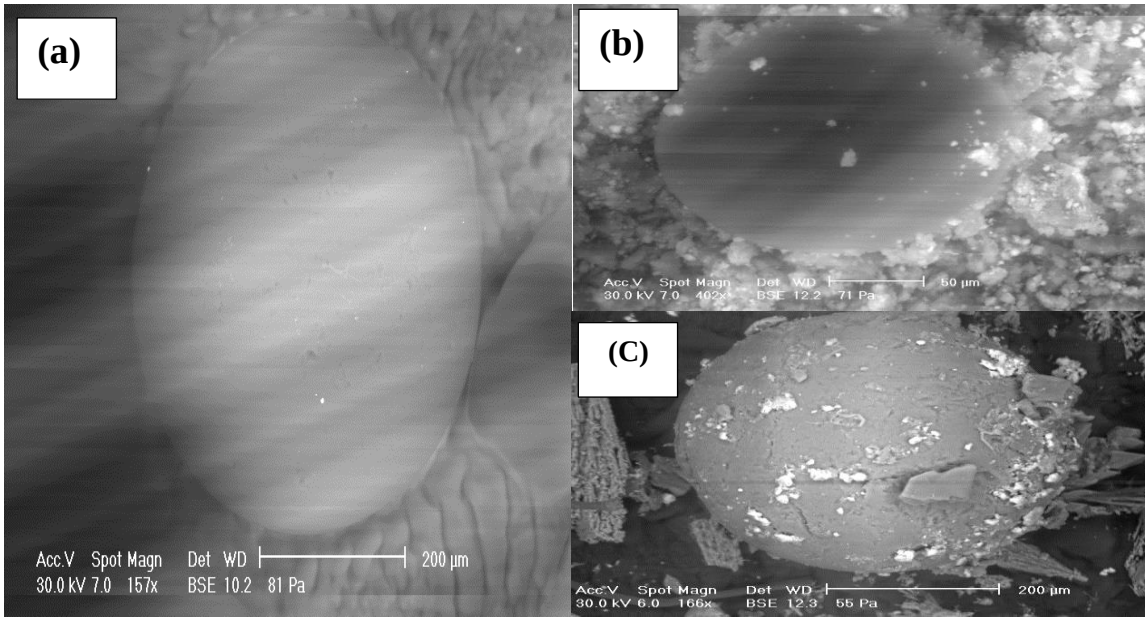

Figure 6. SEM images of resin (a) and U-loaded on resin (b and c).

Effect of temperature

The effect of temperature on uranium adsorption on the resin was studied from 25 to 55°C. The operating conditions involved 100 mL REEs sulfate liquors having 200 U mg / L concentration with initial pH 1.8 using 1 g of adsorbent and contact time of 30 minutes. It can be observed from Fig. 7 that uranium loading has been decreased with increasing temperature may be due to the exothermic nature of U (VI) adsorption in a manner to be favored at room temperature. The uranium adsorption at room temperature (25 ºC) reached 91.2% and decreased down to reach 51.7% at 55 ºC. This decrease in the uranium uptake capacity with increasing temperature might be due to a decreasing effect in the surface activity where at a higher temperature, the thickness of the boundary layer would decrease due to the increasing tendency of U (VI) to escape to the solution phase.

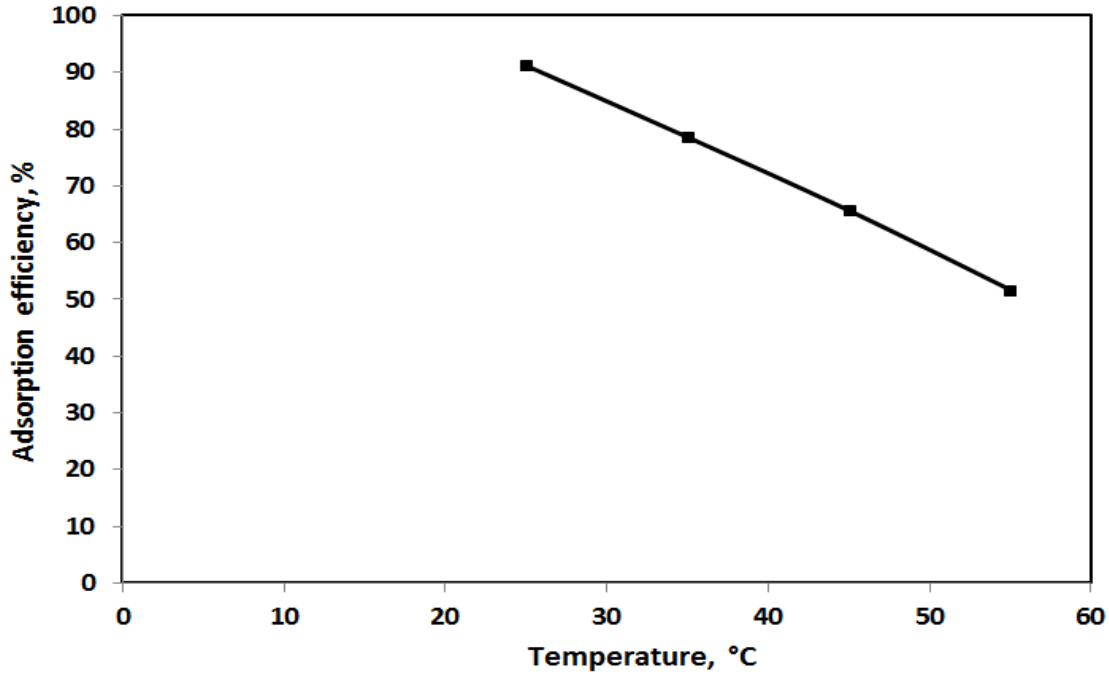

Figure 7. Effect of temperature on adsorption efficiency of lewatit mono plus M500 from REEs sulfate liquor

Interference study

After the dissolution of rare earths concentrate contaminated with uranium in sulfuric acid we found that Rare earths don't interfere or adsorbed on lewatit mono plus M500. This may be due to uranium exists in sulphate solution as anionic complexes $[UO_2(SO_4)_2]^{2-}$ and $[UO_2(SO_4)_2]^{4-}$ which were found to have a high affinity for the anionic exchange resins [39, 40].

In this case, relative adsorption of uranium would occur where other associated impurities of rare earths are present as cations and not therefore allowed for adsorption. Beside the uranyl sulfate complex, some other anions are also adsorbed including ferric sulfate anionic complexes beside chlorate anions [44].

Thermodynamic characteristics

Variations of uranium adsorption data with temperature for uranium adsorption from the REEs sulfate liquor by lewatit mono plus M500 were used to calculate the thermodynamic parameters including the standard enthalpy (ΔH), and the standard entropy (ΔS) based on Van't Hoff plot using the following formula:

$$\ln K_d = \frac{\Delta S}{R} - \frac{\Delta H}{RT} \quad (5)$$

Where K_d is the distribution coefficient ($cm^3\ g^{-1}$), R = 8.3145 J $mol^{-1}K^{-1}$ and T = absolute temperature in Kelvin. ΔH and ΔS were determined from the slope and intercept of ln K_d versus 1/T graph.

Fig. 8 plots ln K_d versus 1/T, K^{-1} which gives a straight line whose slope equals (-ΔH / R) for the adsorption of uranium (VI). The ΔH and ΔS values for uranium (VI) were −61.43 kJ/mol and – 187.37 J/mol k respectively as calculated from the slope and intercept using the Van't Hoff equation.

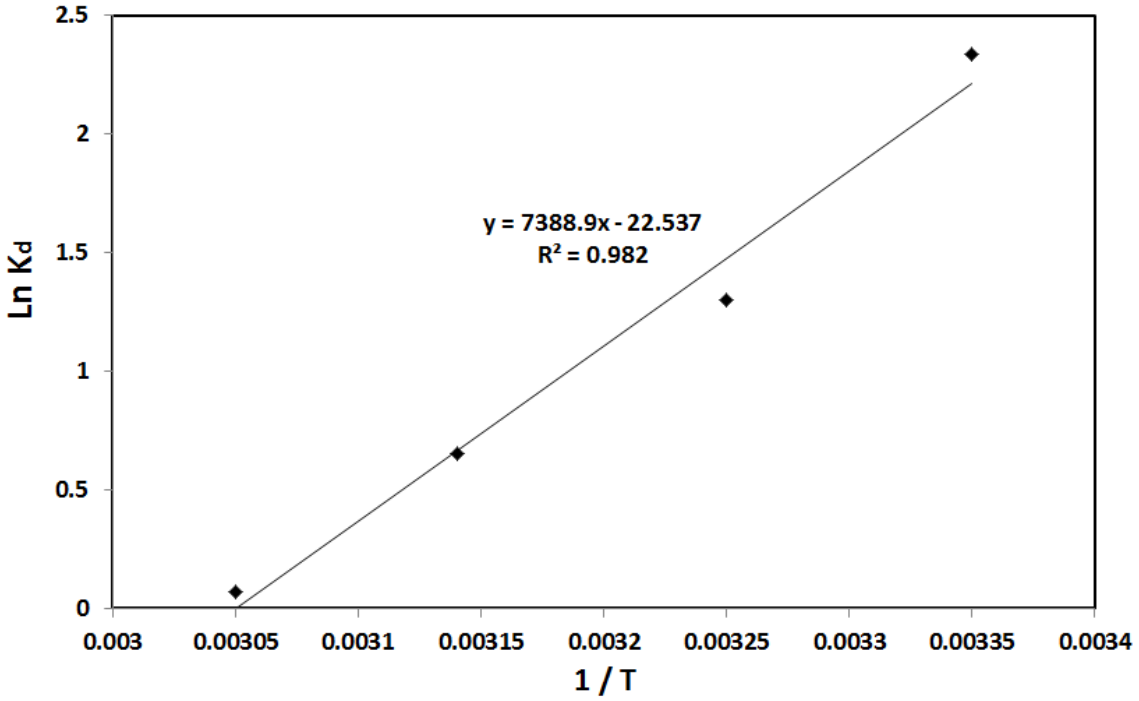

Figure 8. Plot of Ln K_d versus 1/T (K^{-1}) for U adsorption by of lewatit mono plus M500 from the REEs sulfate liquor (200 ppm U)

These values of ΔH and ΔS have then been used to obtain the corresponding free energy (ΔG= − 5.59 kJ/mol) at 298°K using the following equation [45]:

$$\Delta G = \Delta H - T\Delta S \quad (6)$$

The negative value of ΔH indicates that the adsorption of uranium in this system is an exothermic process and that the reaction becomes more favorable at room temperature. The negative value of ΔG indicates that the reaction is spontaneous. On the other hand, the observed decrease in the negative values of ΔG with elevated temperature implies that the reaction becomes more favorable at room temperatures. In addition, the negative ΔS parameter suggests decreasing the system randomness at the solid-liquid interface during the adsorption process.

Kinetic parameters

The kinetic models give indeed important information for designing the sorption process of ranium recovery from its solutions as well as the

rediction of the sorption rate. Fig. 3 gives the sorption capacity of U(VI) of a fixed adsorbent dose of one g which was studied at different contact time periods. It was thus revealed that the U(VI) sorption kinetics by the of lewatit mono plus M500 indicated its rapid binding to the chelating resin sites of the latter during the first few minutes, however this was followed by a slow increase until attaining a state of equilibrium at 30 min with no change in the sorption capacity thereafter till a constant time of 60 min. The initial rapid binding may be due to the availability of a higher number of chelating ion exchange sites in the initial stage followed by a slower sorption due to the gradual decrease in the available chelating ion exchange sites.

The sorption data have then been treated according to the kinetic models of the pseudo-first-order and pseudo-second-order reactions in a manner to study the controlling mechanism of the sorption process. The U(VI) sorption kinetics was thus studied and the experimental data were then tested by the pseudo-first-order equation [46 – 48]; viz:

$$\log (q_e - q_t) = \log q_e - (kt / 2.303) \quad (7)$$

Where q_e and q_t (mg. g^{-1}) are the amounts of U(VI) sorbed at equilibrium and at time t (min), respectively, k_1 is the rate constant of the pseudo-first-order sorption and t (min) is the contact time. The adsorption rate constants (k_1) and the sorption equilibrium capacity (q_e) for the U(VI) sorption by lewatit mono plus M500 were calculated from the slope and intercept of the plots of log (q_e-q_t) against t (Fig. 9) and are reported in Table 3.

It can thus be concluded from the R^2 values that the U(VI) sorption mechanism onto lewatit mono plus M500 does not follow the pseudo-first-order kinetic model and in addition it was found that the experimental equilibrium values of $q_{e,exp}$ (18.24) are not close to the theoretical equilibrium values calculated of $q_{e,cal}$ (8.48) from the above Eq.. Therefore, the pseudo-first-order model is not suitable for modeling the U(VI) sorption onto lewatit mono plus M500 resin. Therefore, the obtained experimental data were tested by the pseudo-second-order kinetic model [46 – 48]; viz:

$$t/q_t = (1/k_2 q_e^2) + (t / qe) \quad (8)$$

Where k_2 (g mg^{-1} min^{-1}) is the rate constant of the pseudo-second-order sorption, q_e (mg g^{-1}) is the sorption capacity at equilibrium and q_t (mg g^{-1}) is the amount of sorption at any time t (min). This model is more likely to predict the kinetic behavior of adsorption with chemical adsorption being the rate-controlling step. The linear plots of t/q_t vs t for the pseudo-second-order model for the U (VI) sorption upon lewatit mono plus M500 at 298 K are shown in (Fig. 10) while the values of the rate constants (k_2), R^2 and q_e are given in Table 3. Based on the correlation coefficients (R^2) (Table 3), the pseudo-second-order kinetic model has actually provided a good correlation for the U(VI) sorption. In addition, there was a close agreement between the calculated equilibrium capacity (19.19) and the experimental equilibrium capacity values (18.24) of q_e confirming the validity of the pseudo-second-order model for explaining the U(VI) sorption mechanism by the prepared lewatit mono plus M500. These results explain that the pseudo-second-order sorption mechanism is predominant and that the overall rate constant of the sorption process appears to be controlled by the chemical sorption process.

Table 3. The kinetic parameters for the U(VI) sorption upon the lewatit mono plus M500 resin.

Parameters	Value	R^2
pseudo-first order		
$q_{e,\,cal.}$ (mg g^{-1})	8.48	
k_1 (min^{-1})	0.0963	0.962
pseudo-second order		
$q_{e,\,cal.}$ (mg g^{-1})	19.19	
k_2 (g mg^{-1} min^{-1})	0.0236	0.998

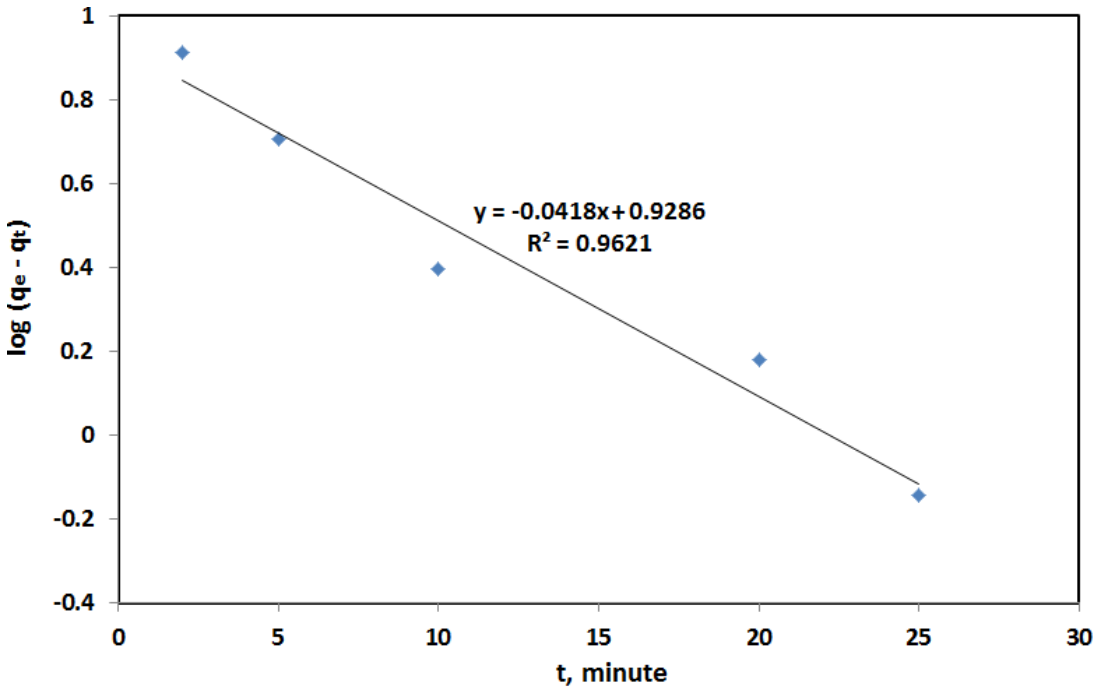

Figure 9. Pseudo-first order kinetics of uranium adsorption on lewatit mono plus M500 resin

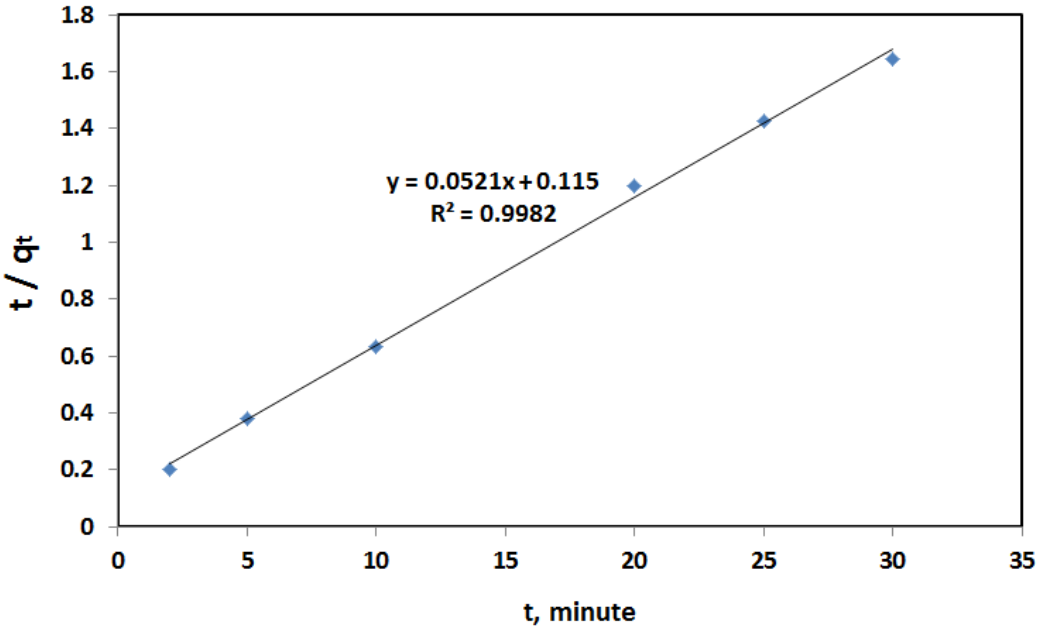

Figure 10. Pseudo-second order kinetics of uranium adsorption on lewatit mono plus M500 resin

Adsorption isotherm study

The adsorption isotherm provides the most important information about how the adsorbed molecules are distributed between the solid and aqueous phases. Adsorption isotherms are most commonly used to select adsorbent and also, they are of great importance for the practical design of adsorption systems [49]. Classical adsorption models (Langmuir and Freundlich) [50 – 53] were used to describe the equilibrium between adsorbed metal ions on the lewatit mono plus M500 (q_{eq}) and that in solution (C_{eq}) at a constant temperature. The Langmuir equation is valid for monolayer sorption on to a surface with a finite number of identical sites and the linearized form is:

$$\mathbf{C_e/q_e = 1/bQ^\circ + C_e/ Q^\circ} \quad (9)$$

Where q_e is the amount of solute sorbed per unit weight of adsorbent (mg g^{-1}), C_e is the equilibrium concentration of the solute in the bulk solution (mg L^{-1}), Q^o is the monolayer saturation adsorption capacity (mg g^{-1}) and b is the Langmuir constants related to adsorption capacity and energy adsorption. The graphic representation of (C_e/q_e) versus C_e gives a straight line for uranium sorbet onto lewatit mono plus M500, Fig. 11, confirming that this expression is a reasonable representation of chemisorption's isotherm. The numerical value of constants Q^o and b evaluated from the slope and intercept of the plot is given in Table 4. The value of saturation capacity Q^o corresponds to the monolayer coverage and defines the total capacity of the adsorbent for uranium. The linearized Langmuir adsorption isotherms of uranium ions obtained at the temperature of 25°C are given in (Fig. 11). From the obtained plotted linear relation, the sorption values and correlation coefficients for U(VI) sorption on the lewatit mono plus M500 have been calculated and are listed in Table 4. From the latter, it is clear that the Langmuir isotherm model provides actually an excellent fit to the obtained equilibrium sorption data giving a correlation coefficient of 0.997 and a maximum adsorption capacity (40.65 mg g^{-1}) close to that experimentally determined (35.5 mg g^{-1}).

One of the essential characteristics of the Langmuir model could be expressed by a dimensionless constant called equilibrium parameters R_L [54]:

$$\mathbf{R_L = 1/(1 + bC_o)} \quad (10)$$

Where C_o is the initial uranium (VI) concentration (mg/L) and K_L is the Langmuir adsorption constant (L/mg). Table 5 lists the calculated results of the R_L values for uranium concentration ranging from 100 to 500 mg/L. Based on the effect of separation factor on the isotherm shape, the R_L values are in the range of $0 < R_L < 1$, which indicates that the adsorption of uranium ions on lewatit mono plus M500 is favorable.

The empirical Freundlich equation based on sorption on a heterogeneous surface is given below as logarithmic form:

$$\mathbf{\log q_e = \log K_f + 1/n \log C_e} \quad (11)$$

K_F and n are the Freundlich constants which represent the adsorption saturation capacity (mg g^{-1}) and the adsorption intensity respectively. K_F and n can be determined from a linear plot of Log q_e against Log C_e (Fig. 12). The numerical values of the constants 1/n and K_f are computed from the slope and intercepts by means of a linear least square fitting method and are given in Table 4 where regression correlation coefficients were found for Freundlich model is 0.889 which means that Langmuir model fit more than Freundlich model in describing sorption equilibrium of uranium by lewatit mono plus M500.

Table 4. Langmuir and Freundlich isotherm model constants applied to uranium sorbed onto lewatit mono plus M500.

Model	Parameters	Value	R^2
Langmuir	Q°(mg/g) b(L/mg)	40.65 0.052	0.997
Freundlich	**K_f (mg/g)** **1/n**	**7.825** **0.322**	0.889

Table 5. The dimensionless separation factor (R_L) for U(VI) ion by lewatit mono plus M500.

C_0	R_L
100	**0.160**
200	**0.087**
300	**0.059**
400	**0.045**
500	**0.037**

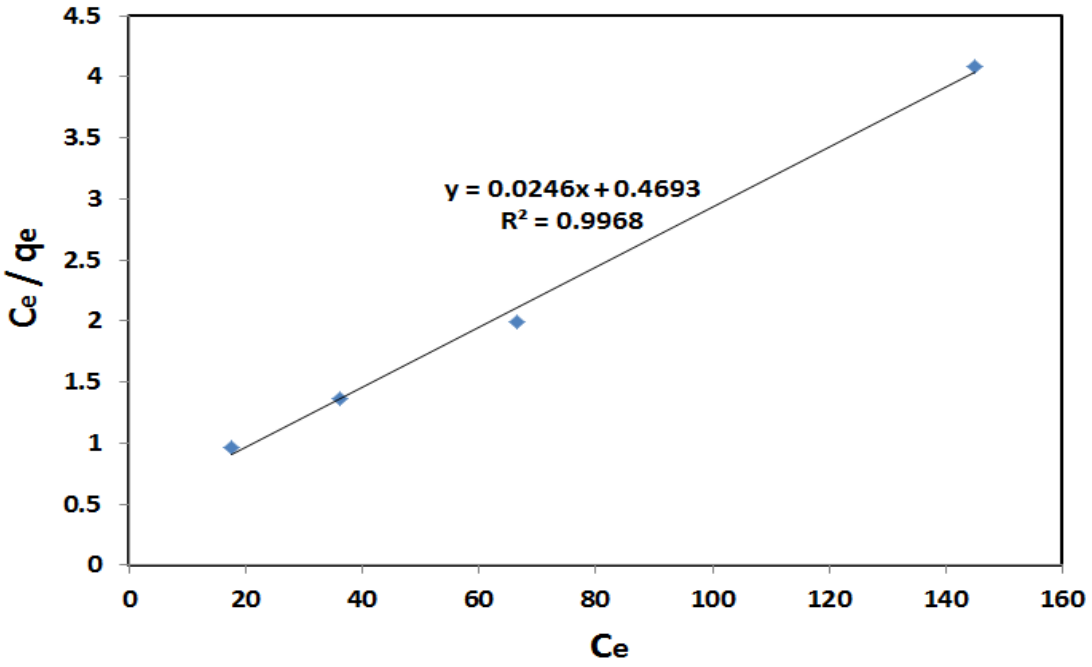

Figure 11. Langmuir isotherm plots for adsorption of uranium onto lewatit mono plus M500

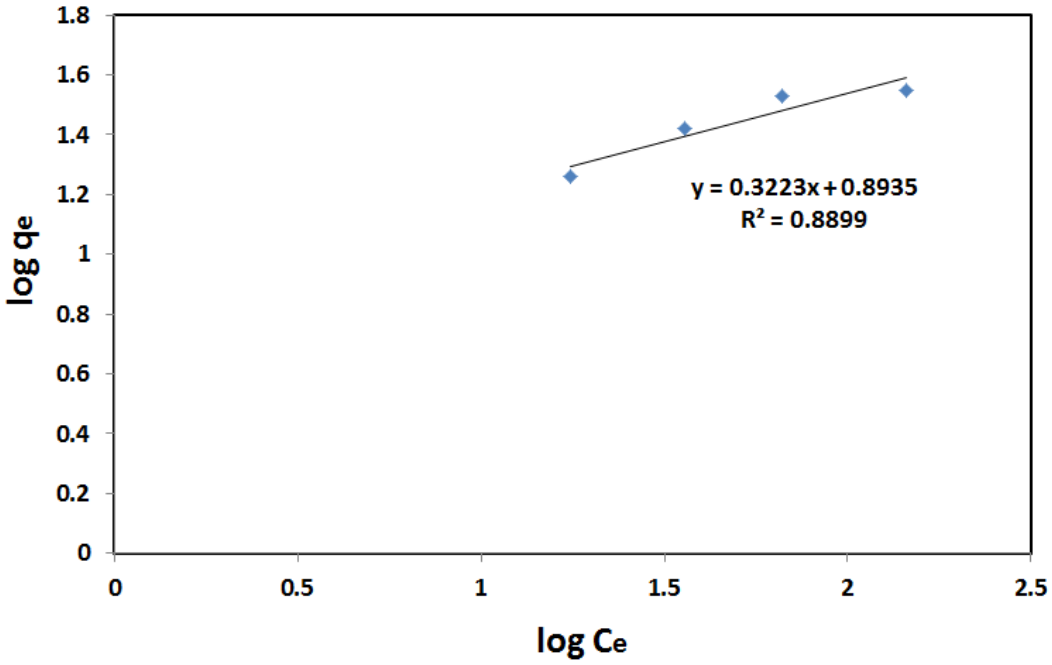

Figure 12. Freundlich isotherm plots for adsorption of uranium onto lewatit mono plus M500

The adsorption capacity Q^o(mg/g) of different adsorbents to adsorb uranium ions as reported in the literature is compared in (Table 6). Comparison of Q^o values shows that lewatit mono plus M500 exhibits a reasonable capacity for uranium adsorption from REEs sulfate solutions.

Table 6. Comparison of the uranium sorption capacity of lewatit mono plus M500 with other sorbents.

Sorbent	Uranium sorption capacity (mg g^{-1})	References
- polyethyl eniminephenyl phosphonamidic acid	**39.66**	[55]
- N`-dimethyl-N,N`-dibutyl malonamide functionalized polymer	**18.78**	[56]
- succinic acid impregnated amberlite XAD-4	**12.33**	[57]
- Gel-amide	**28.98**	[58]
- Gel-benzamide	**18.64**	[58]
- Natural clinoptilolite zeolite	**0.7**	[59]
- Lewatit mono plus M500	**40.65**	This work

Desorption characteristics of the loaded uranium and sorbent regeneration

To enhance the economic value of the sorption process, desorption process was studied. The desorption process will help to regenerate the spent adsorbent so that it can again be reused to adsorb uranium.

Effect of the eluting agent type

Different portions of the resin containing a maximum of adsorbed uranium were equilibrated with various eluents and the results were shown in the following Table 7. In these experiments, the other parameters were kept constant involving a 25mL volume of the eluant solution for 30 minutes contact time at ambient temperature. 2M NaCl + 1M HCl as well as 2M NaCl + 1M H_2SO_4 is found to be efficient eluting agents (99% efficiency).

Table 7. Effect of eluting agent type on uranium elution efficiency from the loaded lewatit mono plus M5.

Eluting agent type	**Uranium elution efficiency %**
HCl (1mole)	53
H_2SO_4 (1mole)	56
1M HCl + 10% Thiourea	60
2M NaCl + 1M HCl	99
2M NaCl + 1M H_2SO_4	99

Effect of molarity 2M NaCl / HCl upon uranium elution efficiency from the loaded lewatit mono plus M500

The concentration effect of both NaCl and HCl on uranium elution from the loaded resin was studied while fixing the other factors constant involving a 25mL volume of the eluant solution for contact time 30 min. at room temperature. From the obtained results given in Table 8, it was obvious that 2M NaCl / 1M HCl acid has resulted in 99% uranium elution efficiency.

Table 8. Effect of NaCl and HCl acid molarity on uranium elution efficiency from the loaded lewatit mono plus M500.

Molarity of NaCl /HCl	**Uranium elution efficiency %**
HCl (1 mole) / NaCl (2 mole)	99
HCl (0.5 mole) / NaCl (2 mole)	82
HCl (0.25mole) / NaCl (2 mole)	52

Effect of elution time

The effect of elution time on uranium elution efficiency was studied in the range from 5-60 min. at the previously studied conditions of optimum molarity of NaCl (2 moles) /HCl (1 mole) at room temperature. The results are given in (Fig. 13). From these results, it was noticed that by increasing the contact time, the elution efficiency increased during the first 30 minutes attaining about 99% of the loaded uranium.

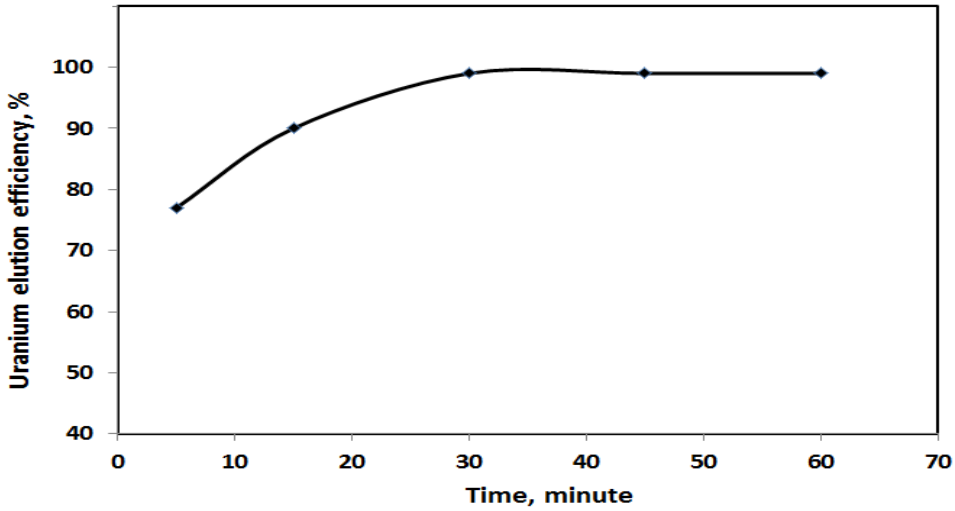

Figure 13. Effect of time on uranium elution efficiency from the loaded lewatit mono plus M500

Durability

To determine the reusability of the Lewatit mono plus M500, consecutive adsorption-desorption cycles were achieved upon the same adsorbent dose using a fresh solution for each cycle under the optimum conditions. From the first to the 20th cycle, it was found that an almost complete uranium adsorption and desorption have been realized. However, behind the latter, the adsorption efficiency of the prepared resin has decreased from 91.2 to 87% in the 25th cycle and also the desorption efficiency has decreased from 99 to 94% in the 25th cycle. Therefore, it would be possible to reuse the resin for about 20 cycles without any noticeable loss of the adsorption capacity indicating that the developed resin matrix has an adequately high mechanical stability in a manner to be recycled for 20 times.

Case study (Up-scaling)

From the above giving, it is evident that the loaded lewatit mono plus M500 resin can be used to separate, purify and concentrate uranium ions from high concentration rare earths sulfate solutions. Therefore, it was tested for this purpose upon the previously prepared rare earth concentrates assaying 200 mg L^{-1} uranium.

The wet rare earth contaminated with uranium (200 ppm), Fig. 14, which produced after sulfuric acid processing of Egyptian monazite was dried and re-dissolved in sulfuric acid.

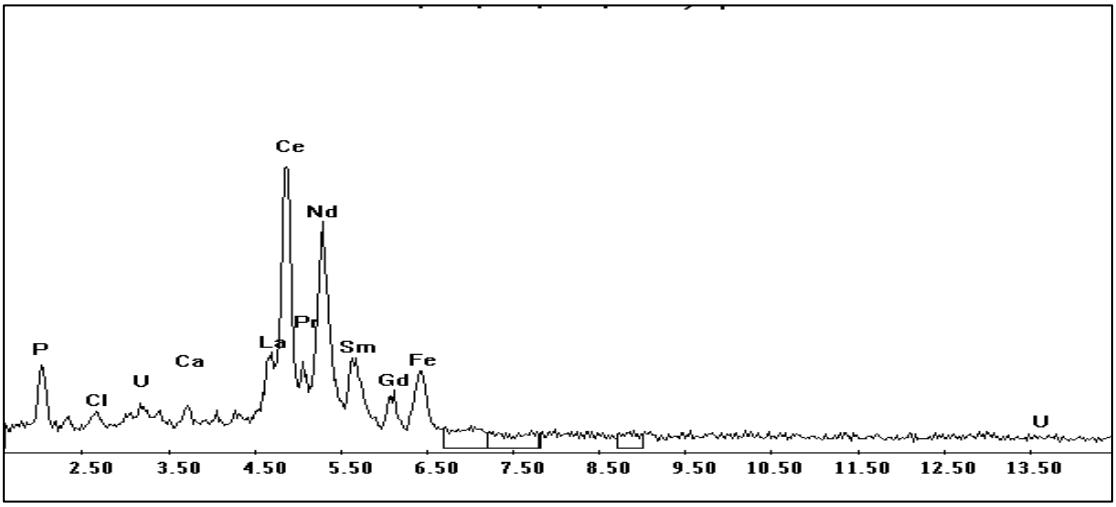

Figure14. EDAX analysis of the contaminated REEs with uranium and other elements

The solution was adjusted to pH= 1.8 and contacted with 1g lewatit mono plus M500 resin under the previously determined optimum conditions. On the other hand, it has also been ascertained that the sorbed U(VI) can be easily desorbed from the uranium-loaded resin using 25 mL NaCl (2 moles) /HCl (1 mole) at room temperature for 30 minutes. The uranium was precipitated from the eluting solution by 10% NaOH and 50% H_2O_2 at pH= 2. The uranium precipitate was dried for 6 hours at 110°C (Fig. 15).

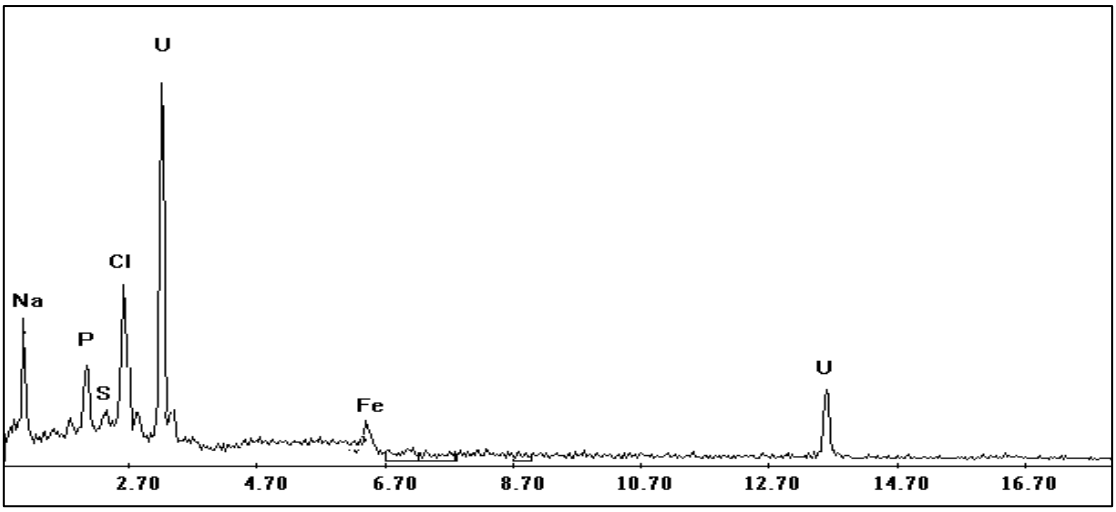

Figure 15. EDAX analysis of the produced uranium concentrate

The rare earths were precipitated from the effluent by oxalic acid to produce REEs oxalate [60] (Table 9 and Fig. 16). A flow diagram was planned as a base for designing a semi-pilot plant as shown in (Fig. 17).

In which a batch of 100 kg hydrated REEs oxide mixture contaminated with maximum 20gram content of uranium has been processed for mutual separation process between REEs mixture & uranium as shown in a pilot skitch (Fig. 18).

Table 9. ICP-OES analysis of REEs produced after purification of crude REEs by adsorption of contaminated uranium with lewatit mono plus M500 resin.

REEs individual	
Element	**%**
La_2O_3	12.7214
Ce_2O_3	27.8430
Nd_2O_3	11.6530
Pr_2O_3	3.1686
Sm_2O_3	2.2157
Eu_2O_3	0.06617
Gd_2O_3	1.5019
Tb_2O_3	0.1316
Dy_2O_3	0.4960
Ho_2O_3	0.0584
Yb_2O_3	0.0529
Tm_2O_3	0.0102
Y_2O_3	1.7532
Er_2O_3	0.0971
Lu_2O_3	0.0058
U_3O_8	N.D
ThO_2	N.D

N.D: means not detected

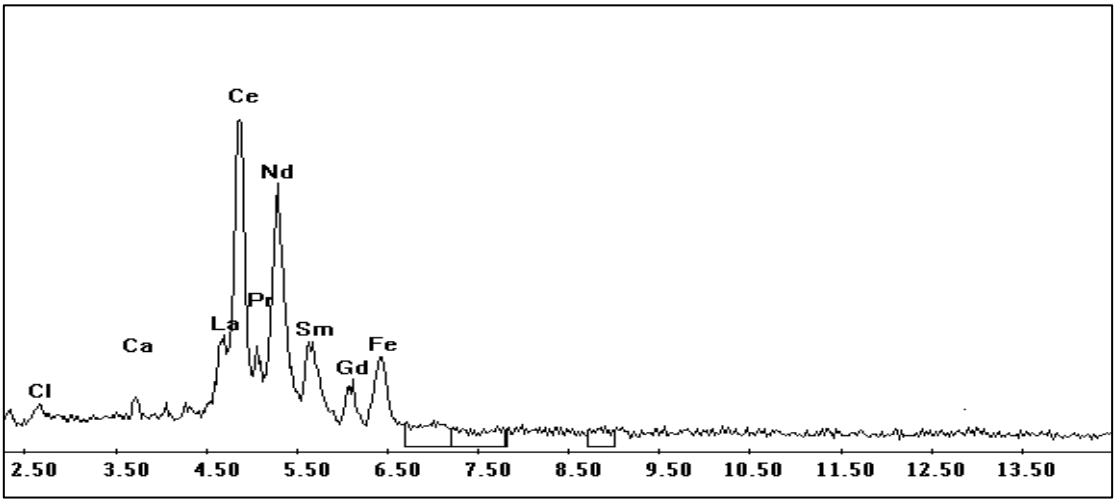

Figure 16. EDAX analysis of the produced rare earth concentrate

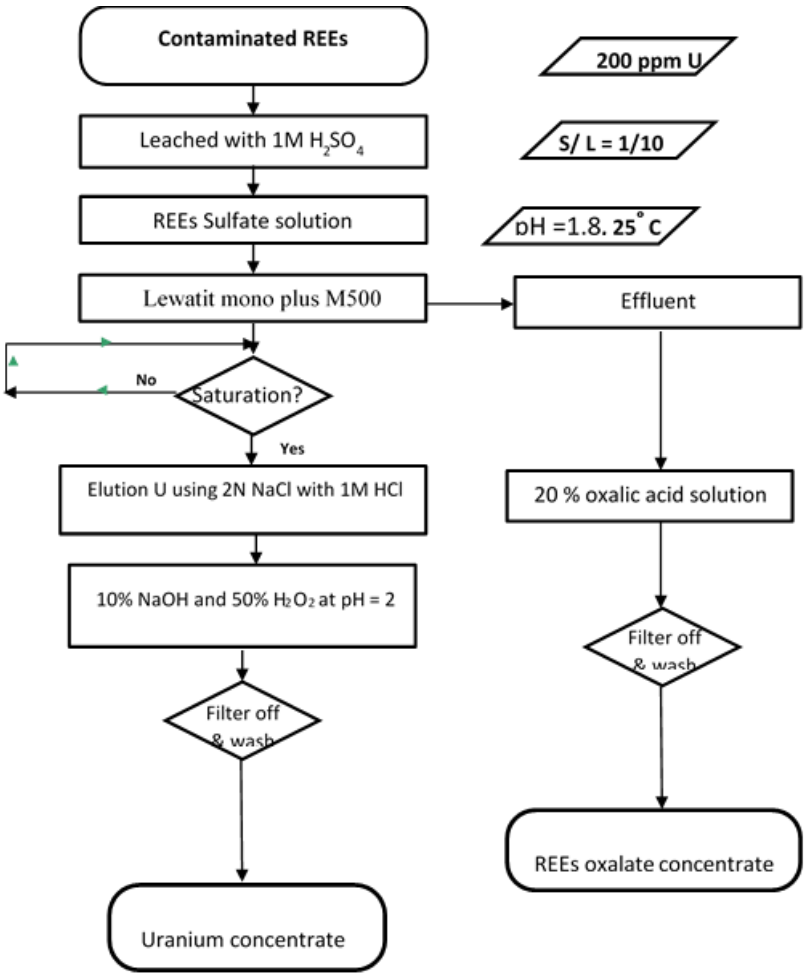

Figure 17. A flow diagram for recovery of uranium from contaminated rare earth using Lewatit mono plus M500.

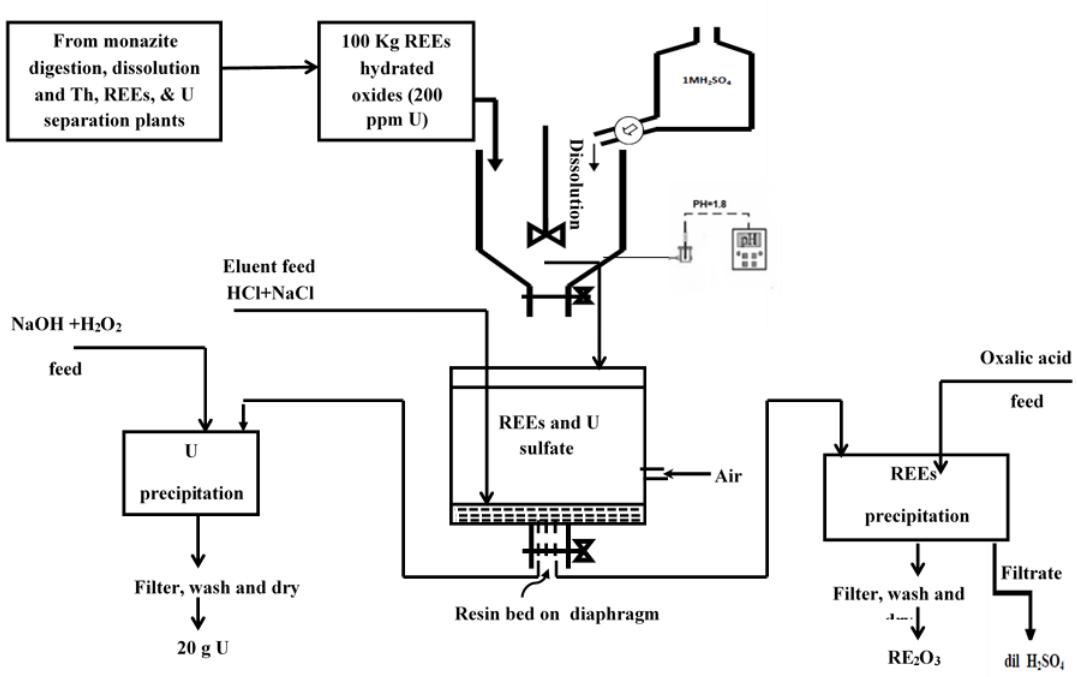

Figure 18. Pilot sketch of 100 g rare earth hydrated oxide treatment for uranium decontamination

Conclusion

A successful adsorption procedure for uranium from rare earths sulfate liquor produced from Egyptian crude monazite has been made possible through application of the lewatit mono plus M500 adsorbent and the studied relevant factors have actually been optimized. It was performed using one g adsorbent of rare earths sulfate liquor (100 mL) contaminated with 200 mg/L uranium at room temperature for 30 min and pH is 1.8. Under these conditions, the achieved uranium capacity was attained 40.65 mg/g. The loaded uranium was afterward completely eluted using 25 mL of 2M NaCl / 1M HCl solution using 30 min contact time for each g of adsorbent. The pseudo-second-order kinetic model was found to be the best fit the experimental results of uranium adsorption by the lewatit mono plus M500 from the rare earths sulfate liquor with a correlation coefficient very close to unity. The effect of temperature data on uranium adsorption by lewatit mono plus M500 resin showed that the enthalpy change is −61.43 kJ/mol indicating its exothermic nature and the reaction is spontaneous. Finally, a marketable product of sodium diuranate was prepared. The rare earths were precipitated from the effluent by oxalic acid to produce REEs oxalate. A proposed pilot unit is suggested for pure salable or REEs production ready for further single REEs separation processes in addition to uranium product.

References

1- D. Harlov, U. Andersson, H. Forster, J. Nystromc, P. Dulski, C. Broman, J. Chem. Geol., 2002, 191, 47-72.
2- Y. El-Nadi, Int.J. *Miner. Process*, 2007, 82, 14-22.
3- W. Kim, I. Bae, S. Chae, H. Shin, H. *J Alloys Compd*, 2009, 486, 610-614.
4- N. Clavier, R. Podor, N. Dacheux, J *Eur Ceram Soc*, 2011, 31, 941-976.
5- A. Jordens, Y. Cheng, K. Waters, *Miner. Eng.*, 2013, 41, 97-114.
6- F. Xie, T. Zhang, D. Dreisinger, F. Doyle, *Miner. Eng.*, 2014, 56, 10-28.
7- G. Liu, X. Chen, Spectroscopic properties of lanthanides in nanomaterials, 2007 In: K. Gschneidner, Jr. Bünzli, V. Pecharsky (Eds.), *Handbook on the Physics and Chemistry of Rare Earths*, 37, pp. 99–169.
8- L. Chi, J. Tian, *Journal of the Chinese Rare Earth Society*, 2007, 25 (6), 641-652 (in Chinese).
9- R. Yang, W. Wang, X. Zhang, L. Liu, H. Wei, M. Bao, J. Wang, *J RARE EARTH*, 2008, 26 (5), 753-759.
10- G. Wang, *Si Chuan Rare Earth*, 2009, 3, 4 -7 (in Chinese).
11- G. Wang, *Si Chuan Rare Earth*, 2006, 3, 2-8 (in Chinese).
12- G. Wang, J. Tang, 2007 In: Proceedings of the Conference for Chinese Rare Earth Comprehensive Exploitation and Environment Protection. June 6–10, Haikou, Hainan China, 147–153 (in Chinese).
13- Y. Anwar, A. Abdel-Rehim, *Bull. Fac. Sci. Alex. Univ.*, 1970, 10, 152-171.
14- G. Dabbour, Estimation of economic minerals reserves in Rosetta beach sands, Egypt. Min. J., 1995, 7, 153 - 166.
15- C. Gupta, N. Krishnamurthy, *Extractive Metallurgy of Rare Earths*, CRC Press, New York, 2004.

16- E. Kim, K. Osseo-Asare, *Hydrometallurgy*, 2012, 113-114, 67-78.
17- R. Panda, A. Kumari, M. Jha, J. Hait, V. Kumar, J. Kumar, J. Lee, *J. Ind Eng Chem*, 2014, 20, 2035-2042.
18- I. Rojkovic, J. Medved, E. Walzel, *Geologicky Zbornik Geologica*, 1989, 40, (4), 453-469.
19- C. Tsai, S. Yeh, J. *Radioanal. Nucl. Chem.*, 1997, 216 (2): 241 – 245.
20- A. Paul, P. Pillai, S. Horidasan, S. Radhakrishnam, *J. Environ. Radioactivity*, 1998, 40 (3), 251-259.
21- H. Song, M. Hong, The analysis and prediction of rare earth industry in China (I), Rare Earth, Information, 2010, No.2, 6–8 (in Chinese).
22- F. Xu, L. Zhang, X. Dong, Q. Liu, M. Komuro, *Scr Mater*, 2011, 64, 1137-1140.
23- D. Tu, Y. Liang, R. Liu, D. Li, *J Lumin*, 2011, 131, 2569-2573.
24- S. Ye, F. Xiao, Y. Pan, Y. Ma, Q. Zhang, *Mater Sci Eng*, 2011, R 71, 1-34.
25- E. Karsu, E. Popovici, A. Ege, M. Morar, E. Indrea, T. Karali, N. Can, *J Lumin*, 2011, 131, 1052-1057.
26- K. Soldenhoff, Challenge in rare earth processing, In: ALTA 2013 Uranium-REE Conference. May 25–June 1, Perth, Western Australia, 2013.
27- G. Lapidus, F. Doyle, *Hydrometallurgy*, 2015, 154, 102-110.
28- N. Abdelfattah, A. Abdou, A. Bakry, *J Appl Sci Res*, 2014, 1(1), 22-29.
29- J. Ganser, A. Napier, J. Kyle, D.White, S. Jayasekera, The Nolans rare earth project-an update., ALTA 2014 Uranium-Rare earth conference, May 24–31,2014, Perth, Australia.
30- G. Lockyer, Bridging the rare earths gap. In: Rare Earths North America 2014 Conference, June 11, 2014, New York City, USA.
31- C. Gupta, H. Singh, Uranium Resource Processing: Secondary Resource, Heidelberg 2003. Springer-Verlag Berlin, Germany.
32- A. Zamani, M. Yaftian, Sep. *Purif. Technol*., 2004, 40, 115-121.
33- J. Preston, A. du Preez, *Solvent Extr. Ion Exch*., 1995, 13 (3), 391-419.
34- P. Kewsuwan, Proceeding of the 6th Conference on Nuclear Science and Technology, 1996, 761, 31.K. Rabie, Y. AbdelMoneam, A. Abd El-Fatah, M. Demerdash, A. Salem, *international journal of research in engineering and technology*, 2014, 3(6), 374-382.
35- L. Shapiro, N. Brannock, Rapid analysis of silicate, carbonate and phosphate rocks, United States Geological Survey Bulletin, 1962, 114 A, 65.
36- Z. Marczenko, Spectrophotometric determination of elements, New York: John Wiley and Sons, 1986.
37- M. Avila, T. Burks, F. Akhtar, M. Göthelid, P. Lansåker, M. Toprak, M. Muhammed, A. Uheida, *Chem. Eng. J*., 2014, 245, 201-209.
38- A. Suner, A. Lagos, Recovery of uranium from the Malargue, Merdoza, Mineral by ionic exchange, Proc. Int. Conf. on the Peac. Uses of At. Energy, Geneva, Vol.3, 1958.
39- F. Nachod, J. Schubert, Ion Exchange Technolgy, Academic Press Inc. Publishers New York, 1956.
40- G. Sheng, J. Sheng, S. Yang, J. Hu, X. Wang, *J Radioanal. Nucl. Chem*., 2011, 289(1), 129-135.
41- J. Hu, Z. Xie, B. He, G. Sheng, C. Chen, J. Li, Y. Chen, X. Wang, *Sci China B*, 2010, 53(6), 1420.
42- L. Fan, Y. Zhang, C. Luo, F. Lu, H. Qiu, M. Sun, *Int.J.Biol.Macromol*., 2012, 50(2), 444-450.
43- A. Preuss, R. Kunin, A general survey of types and characteristics of ion exchange resins used in uranium recovery, Peaceful Uses of Atomic Energy (Proc. Int. Conf. Geneva, 1955), Vol. 8, United Nations, New York, 1956, 45-58.
44- A. El-Nadi, A. Daoud, *J Radioanal. Nucl. Chem*., 2005, 265, 447-454.
45- G. McKay, Y. Ho, *Resour. Conserv. Recycling*., 1999a, 25, 171-193.
46- G. McKay, Y. Ho, *J. Water Res*., 1999b, 33, 587-584.
47- G. McKay, Y. Ho, *J. Process Biochem*., 1999c, 34, 451-465.
48- S. Yusan, S. Akyil Erenturk, *Desalination*, 2010, 263, 233-239.
49- I. Langmuir, *J. Am. Chem. Soc*., 1918, 40 (9): 1361–1403, doi: http://dx.doi.org/10.1021/ja02242a004.
50- E. El-Sofany, W. Zahera, H. Aly, *J. Hazard. Mater*., 2009, 165, 623-629.
51- S. Giffin, A. Davis, *J Environ Eng*, 1998, 12(10), 921-931.
52- H. Freundlich, Adsorption in solution, *Physical and Chemical Society*, 1906, 40, 1361-1368.
53- D. Mohan, S. Chander, *J. Colloid Interf. Sci*., 2006, 299, 57-76.
54- O. Abderrahim, M. Didi, D. Villemin, *J Radioanal. Nucl. Chem*., 2009, 279(1), 237-244.
55- SA. Ansari, PK. Mohapatra, VK. Manchanda, *J. Hazard. Mater.*, 2009, 161(2–3), 1323-1329.
56- P. Metilda, K. Sanghamitra, J. Mary Gladis, G. Naidu, T. Prasada Rao, *Talanta*, 2005, 65(1), 192-200.
57- K. Venkatesan, V. Sukumaran, M. Antony, P. Vasudeva Rao, *J. Radioanal. Nucl.Chem.*, 2004, 260(3), 443-450.
58- L. Camacho, S. Deng, R. Parra, *J. Hazard. Mater*., 2010, 175(1–3), 393-398.
59- E. Borai, M. Abd El-Ghany, I. Ahmed, M. Hamed, A. Shahr El-Din, H. Aly, *Int.J. Miner. Process*, 2016, doi: 10.1016/j.minpro.2016.02.